

Gene expression profiling of hypoxia signaling in human hepatocellular carcinoma cells

A. Vengellur, J. M. Phillips, J. B. Hogenesch and J. J. LaPres

Physiol. Genomics 22:308-318, 2005. First published Jun 7, 2005;

doi:10.1152/physiolgenomics.00045.2004

You might find this additional information useful...

Supplemental material for this article can be found at:

<http://physiolgenomics.physiology.org/cgi/content/full/00045.2004/DC1>

This article cites 33 articles, 17 of which you can access free at:

<http://physiolgenomics.physiology.org/cgi/content/full/22/3/308#BIBL>

This article has been cited by 1 other HighWire hosted article:

Physiological genomics in PG and beyond: July to September 2005

M. Liang and B. Ventura

Physiol Genomics, October 17, 2005; 23 (2): 119-124.

[Full Text] [PDF]

Updated information and services including high-resolution figures, can be found at:

<http://physiolgenomics.physiology.org/cgi/content/full/22/3/308>

Additional material and information about *Physiological Genomics* can be found at:

<http://www.the-aps.org/publications/pg>

This information is current as of November 17, 2005 .

Gene expression profiling of hypoxia signaling in human hepatocellular carcinoma cells

A. Vengellur,^{1,2} J. M. Phillips,¹ J. B. Hogenesch,³ and J. J. LaPres^{1,4,5}

¹Department of Biochemistry and Molecular Biology and ²Graduate Program in Genetics, Michigan State University, East Lansing, Michigan; ³The Genomics Institute of the Novartis Research Foundation, San Diego, California; and ⁴National Food Safety and Toxicology Center and ⁵Center for Integrative Toxicology, Michigan State University, East Lansing, Michigan

Submitted 20 February 2004; accepted in final form 2 June 2005

Vengellur, A., J. M. Phillips, J. B. Hogenesch, and J. J. LaPres. Gene expression profiling of hypoxia signaling in human hepatocellular carcinoma cells. *Physiol Genomics* 22: 308–318, 2005. First published June 7, 2005; 10.1152/physiolgenomics.00045.2004.—Cellular, local, and organismal responses to low O₂ availability occur during processes such as anaerobic metabolism and wound healing and pathological conditions such as stroke and cancer. These responses include increases in glycolytic activity, vascularization, breathing, and red blood cell production. These responses are mediated in part by the hypoxia-inducible factors (HIFs), which receive information on O₂ levels from a group of iron- and O₂-dependent hydroxylases. Hypoxia mimics, such as cobalt chloride, nickel chloride, and deferoxamine, act to simulate hypoxia by altering the iron status of these hydroxylases. To determine whether these mimics are appropriate substitutes for the lower O₂ tension evoked naturally, we compared transcriptional responses of a Hep3B cell line using high-density oligonucleotide arrays. A battery of core genes was identified that was shared by all four treatments (hypoxia, cobalt, nickel, and deferoxamine) including glycolytic enzymes, cell cycle regulators, and apoptotic genes. Importantly, cobalt, nickel, and deferoxamine influenced transcription of distinct sets of genes that were not affected by cellular hypoxia. These global responses to hypoxia indicate a balancing act between adaptation and programmed cell death and suggest caution in the use of hypoxia mimics as substitutes for the low O₂ tension that occurs in vivo.

Affymetrix array; Hep3B; genomics; hepatocellular carcinoma

CELLS, TISSUES, AND ORGANISMS are said to be hypoxic when they receive less than normal levels of oxygen. Given the central role of oxygen in the production of ATP through oxidative phosphorylation, it is critical for cells and tissues to respond rapidly to hypoxia. The importance of hypoxia signaling is further highlighted by its essential role in mammalian development and several pathological conditions such as cardiovascular disease and cancer (4). The primary response to hypoxia within the cell is the upregulation of proteins and pathways such as glycolytic enzymes and angiogenic factors that ultimately lead to alternative routes of ATP generation and an increased oxygen availability (10). Glycolytic enzymes that are targets for such upregulation include glyceraldehydes-3-phosphate dehydrogenase (GAPDH), pyruvate kinase, and phosphofructokinase (27). At the tissue level, there is a stimulation of angiogenesis through the upregulation of growth factors such as vascular endothelial growth factor (VEGF) (19). These

responses and others are regulated by a family of transcription factors called the hypoxia-inducible factors (HIFs).

HIFs are members of the bHLH-PAS (basic-helix-loop-helix-PER, ARNT, SIM) family of transcription factors (12). There are three cytosolic HIFs: HIF1 α , HIF2 α , and HIF3 α . The most studied of these is HIF1 α . Under normoxic conditions, HIF1 α is ubiquitously transcribed, translated, and subsequently degraded. Under hypoxic conditions, however, HIF1 α protein becomes stabilized (2, 16, 26). This oxygen-dependent degradation of the HIF1 α protein is primarily controlled by a family of nonheme oxygenases called prolyl hydroxylase domain-containing proteins (PHDs, also known as HIF prolyl hydroxylases) (3, 6). There are three PHDs in mammals, and recent reports suggest that they have differing cellular localization and regulatory activities on HIF1 α (1, 21). These hydroxylases may also participate in feedback inhibition, since they themselves are hypoxia-regulated genes. (5, 21, 32) The PHDs use oxygen as a cosubstrate and are dependent on iron and 2-oxoglutarate for function (23). In the presence of oxygen, these enzymes are capable of hydroxylating proline residues within the oxygen-dependent degradation domains (ODDs) of HIF1 α . Once hydroxylated, the ODD becomes an interaction surface for the Von Hippel Lindau tumor suppressor (VHL), which binds the HIF1 α protein, recruits the ubiquitination machinery, and ultimately leads to HIF1 α degradation in a proteasome-dependent fashion (17). The iron-dependent activity of the PHD enzymes may help explain the ability of iron chelators and divalent metals to promote a hypoxic-like response. In fact, cobalt chloride and nickel chloride, transition metals capable of competing with iron at binding sites, and deferoxamine, an iron chelator, are widely used as hypoxia mimics. The appropriateness of these hypoxia mimics has not been thoroughly tested.

Under hypoxic conditions, HIF1 α is stabilized and translocates to the nucleus where it dimerizes with its partner, the aryl hydrocarbon nuclear translocator (ARNT, also known as HIF1 β) (16). The HIF1 α :ARNT heterodimer, referred to as HIF1, recognizes specific sequences within the genome, termed hypoxia-responsive elements (HREs), and, on binding of these sites in the appropriate context, the complex becomes transcriptionally active (2, 26). While >50 HIF1 α -responsive genes have been characterized, the pleiotropic responses to hypoxia suggest the existence of unidentified hypoxia-responsive genes. Furthermore, although widely used as hypoxia mimics, the suitability of cobalt, nickel, and deferoxamine as hypoxia analogs has not been comprehensively addressed. These current studies were performed to characterize a more complete battery of hypoxia-regulated genes and to determine whether cobalt chloride, nickel chloride, and deferoxamine are

Article published online before print. See web site for date of publication (<http://physiolgenomics.physiology.org>).

Address for reprint requests and other correspondence: J. J. LaPres, 402 Biochemistry Bldg., Michigan State Univ., East Lansing, MI 48824-1319 (e-mail: lapres@msu.edu).

Table 1. Primers used in qRT-PCR

Gene	Accession No.	Forward	Reverse
HPRT	NM_000194	gaccagtcacacaggggacat	cctgaccaagaaaagcaaaag
VEGF	AF024710	tcctcacaccattgaaacca	gatcctgcctctctctctg
HumIP (IP30)	BC031020	tgcaaatcaacaagggtgga	gcaggcatagtgccagactt
SLC6A8	NM_005629	ctggaaactctgtcccctgt	cagcgtggtgtaaaagact
PDK1	NM_002610	ttcggatcagtggaatgctg	accaattgaacggatggtgt
Carb. Annh. (MaTu)	NM_001216	acttcagccgctacttccaa	agagggtgtggagctgctta
IL8	M28130	tagccaggatccacaagtcc	gctccacatgtcctcaca
HGFAL	NM_004132	cctctctaccctcccacaag	cgctggatagacagctctgc
Inhibin	NM_002193	aaggacacaaccctgcagag	tttagccctctctctctcc
MAOA	NM_000240	acataaggagttgcccgata	agcatttcccacaaagggtg
MCT3	NM_004207	acaactgagctggtcagg	ctctggaatgacacggtcc
15-PGDH	NM_000860	tggtgaaaactctttgcaagc	agctgggaggtctggagitta
Cyp11a1	NM_000499	ctccgacactctctctg	ggtgatctgccactggttt

qRT-PCR, quantitative RT-PCR.

appropriate hypoxia mimics. To address these goals, the hepatocellular carcinoma cell line, Hep3B, was exposed to hypoxia, cobalt chloride, nickel chloride, or deferoxamine (DFO); total RNA was extracted; and transcriptional responses were

evaluated using high-density oligonucleotide arrays. Comparisons among the four treatments suggest that there is substantial overlap; however, there is also a large set of genes that are specific for the individual treatments. Several genes involved in creatine transport and pyruvate metabolism were shown to be general responders to all treatments. In addition, several protooncogenes, kinases, cell cycle regulators, and hydroxylases have also been found to be regulated by hypoxia.

MATERIALS AND METHODS

Cell culture. Hep3B cells were maintained in MEM (Invitrogen) supplemented with 10% fetal bovine serum (Hyclone, Logan, UT), 20 mM L-glutamine, 1 mM MEM nonessential amino acids, 100 mM HEPES (pH 7.4), 1,000 U/ml penicillin G, and 1,000 µg/ml streptomycin sulfate (Invitrogen). Cells were ~70% confluent at the time of treatment. Cells were maintained at 37°C, 5% CO₂, and 21% O₂ before treatment. Hypoxia treatment (1% O₂) was performed in an O₂-regulated incubator (Precision-NAPCO 7000; Winchester, VA) at 37°C and 5% CO₂. Cobalt chloride (100 µM), nickel chloride (100 µM), and DFO (100 µM) treatments were performed at 37°C, 5% CO₂, and 21% O₂.

Table 2. Top 20 hypoxia up- and downregulated probe sets

Probe Set	Fold Change				Descriptions
	HYP	COB	DFO	NICK	
39352_at	-13.1	-1.9	2.5	-6.7	thyroid-stimulating hormone alpha subunit
1025_g_at	-10.2	-5.9	-14.7	-8.2	HSCYP450 human gene for cytochrome P(1)-450
32570_at	-6.9	-5.8	-7.3	-5.4	15-hydroxyprostaglandin dehydrogenase (PGDH)
742_at	-5.0	-9.6	-4.4	-11.4	human mRNA for HGF activator like protein
40588_r_at	-4.7	1.0	-4.8	-2.9	p18 protein
41363_at	-4.7	-1.7	-6.4	-2.6	survival of motor neuron protein interacting protein 1
39382_at	-4.5	-1.5	-3.4	-2.2	mRNA for KIAA0517 gb = AB011089
36592_at	-4.5	-1.5	-8.3	-2.6	prohibitin
38680_at	-4.4	-1.4	-1.6	-2.0	Alu repeats, region 5 to the SNRP E gene
39355_at	-4.3	-1.4	-6.5	-2.6	2-5A binding protein
31880_at	-4.1	-1.4	-6.6	-3.5	N9 Rep-8 gb = D83767
36636_at	-4.0	1.0	1.1	-1.9	omithine aminotransferase
41772_at	-4.0	-2.2	-4.7	-2.9	monoamine oxidase A
38323_at	-4.0	1.1	-7.1	-2.8	BAC clone RG113D17 gb = AC005162
33791_at	-3.9	1.9	-2.6	-2.3	leukemia associated gene 1
38372_at	-3.9	-1.1	-1.7	-2.6	U66042:Human clone 191B7
40788_at	-3.9	1.0	-1.3	-2.6	adenylate kinase 2A (AK2A)
1969_s_at	-3.8	-1.0	-1.8	-2.9	CDK activating kinase
41246_at	-3.7	-1.4	1.8	-3.9	<i>Homo sapiens</i> gb = AI743134
37297_at	-3.7	-1.4	-3.7	-2.4	<i>Homo sapiens</i> DKFZp586A191
37758_s_at	4.6	-1.1	4.8	4.5	<i>Homo sapiens</i> gb = W28479
39827_at	4.7	4.4	4.7	6.8	<i>Homo sapiens</i> gb = AA522530
36386_at	4.7	10.8	14.9	3.9	pyruvate dehydrogenase kinase isoenzyme 1
40790_at	4.9	4.0	8.0	4.2	DEC1
36101_s_at	5.0	3.6	7.2	4.1	vascular endothelial growth factor
38545_at	5.2	2.5	12.1	4.0	testicular inhibitor beta-B-subunit
40926_at	5.8	12.1	25.5	6.7	creatine transporter (SLC6A8)
38125_at	6.3	10.6	22.8	7.9	plasminogen activator inhibitor I
HUMGAPDH	6.5	-1.0	2.9	2.7	glyceraldehyde-3-phosphate dehydrogenase
40888_f_at	6.6	-1.3	3.6	3.3	<i>Homo sapiens</i> gb = W28170
34777_at	6.8	33.1	39.4	3.9	adrenomedullin precursor
32588_s_at	7.0	-2.5	1.3	8.5	ERF-2
40309_at	8.1	39.4	39.9	5.7	carbonic anhydrases (MaTu MN)
31918_at	8.4	1.2	9.0	5.5	homeodomain protein (Prox 1)
34610_at	8.6	-1.0	1.6	3.1	<i>Homo sapiens</i> gb = W25845
1591_s_at	11.9	2.2	8.6	8.5	insulin-like growth factor II
36782_s_at	13.9	2.3	10.3	13.2	insulin-like growth factor II
672_at	14.2	7.4	13.5	3.3	plasminogen activator inhibitor-1
36933_at	79.9	127.7	241.0	61.5	RTP (N-myc downstream regulated gene 1)
2079_s_at	255.6	27.6	140.0	202.7	insulin-like growth factor (IGF-II)

HYP, hypoxia; COB, cobalt; DFO, deferoxamine; NICK, nickel.

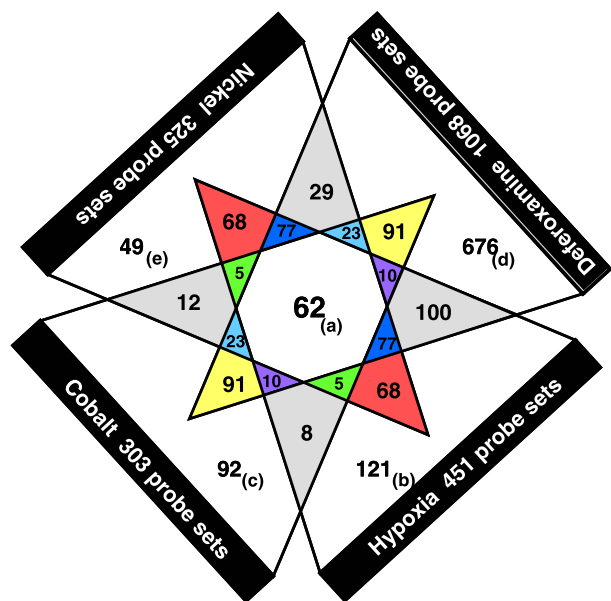


Fig. 1. Venn diagrams representing genes the expression of which was significantly influenced by treatment. Genes whose expression was influenced by the 4 hypoxia treatments are displayed as Venn diagrams. Total no. of genes for each treatment group is listed at the *bottom* next to the treatment label. Each section that shares the same color and no. represents the same subset of genes. *a*: A complete list of these genes can be found in Table 3. *b*: A partial list of these genes can be found in Table 4. *c*: A partial list of these genes can be found in Table 5. *d*: A partial list of these genes can be found in Table 6. *e*: A partial list of these genes can be found in Table 7. All genes for each treatment can be found in the Supplemental Materials (see *footnote 1*).

RNA extraction. RNA was extracted by homogenization (Polytron; Kinematica, Lucerne, Switzerland) in TRIzol reagent (Gibco BRL) (added to cell pellet) at maximum speed for 90–120 s. The homogenate was allowed to incubate for 5 min at room temperature, a 1:5 volume of chloroform was added, and the tube was vortexed and, finally, subjected to centrifugation at 12,000 *g* for 15 min. The aqueous phase was isolated, and a one-half volume of isopropanol was added to precipitate the RNA. After this initial isolation, a secondary purification was performed with the Qiagen RNeasy Total RNA isolation kit according to manufacturer's specifications. The purified total RNA was finally eluted in 10 μ l of diethyl pyrocarbonate-treated H₂O, and quantity and integrity were characterized using a Beckman DU640 UV spectrophotometer and Agilent Bioanalyzer 2100.

RNA labeling. Briefly, 5 μ g of total RNA from two separate biological replicates were used to make first-strand cDNA using the Superscript Choice system (Gibco BRL) and a T7 promoter/oligo(dT) primer (Gibco). Second-strand cDNA was also made with the Superscript Choice system. The resulting cDNA was subjected to phenol-chloroform purification and ammonium acetate precipitation, and used as a template to make biotinylated amplified antisense cRNA using T7 RNA polymerase (Enzo kit, Affymetrix). Twenty micrograms of cRNA were fragmented to a range of 20–100 bases in length using fragmentation buffer (200 mM Tris-acetate, pH 8.1, 500 mM potassium acetate, 150 mM magnesium acetate) and heating for 35 min at 94°C. The quality of cRNA and size distribution of fragmented cRNA were examined by both agarose and polyacrylamide gel electrophoresis.

Hybridization. Twenty micrograms of cRNA were hybridized to a U95A version 1 gene chip (Affymetrix) with 1 \times MES hybridization buffer using standard protocols outlined in the Gene Chip Expression Analysis Technical Manual (Affymetrix). Hybridization was conducted in a GeneChip hybridization oven for 16 h at 45°C. After

hybridization, the arrays were washed on a GeneChip Fluidics Station 400 according to the manufacturer's instructions (Affymetrix). The arrays were scanned using a Hewlett-Packard 2500A Gene Array Scanner, and the raw images were visually scanned for defects and proper grid alignment and converted into CEL files using the MAS5 Software Suite (Affymetrix). Finally, quality of cRNA was assessed by examining 3'-to-5' ratios for GAPDH oligonucleotides present on the arrays.

Data analysis. Background subtraction and single-intensity measures for each transcript were arrived from multiple probe sets by means of the GCRMA algorithm, using the "full model tag" in R (<http://www.r-project.org>) (9, 15, 33). The GCRMA algorithm was chosen for its much improved performance in reporting low- and high-level expression over other methods as well as its dynamic range for single probe sets. Differentially expressed genes that are statistically significant were determined by ANOVA. Fold-change calculations were performed in Excel on data that were median scaled to a global intensity target value of 100. For each treatment vs. control condition, genes that changed were assigned based on a *P* value of <0.05 and a fold change value of >2. The microarray data have been uploaded to the Gene Expression Omnibus (GEO) database (series no. GSE1056 and sample nos. GSM17082–GSM17097, GSM48163, and GSM48164).

Quantitative real-time PCR analysis. Changes in gene expression observed by microarray analyses were verified by real-time PCR, performed on an Applied Biosystems Prism 7000 sequence detection system (Foster City, CA) as described (32). Briefly, cDNA was synthesized from total RNA (1 μ g per sample per treatment, *n* = 6) in a reverse transcriptase (RT) reaction in 20 μ l of 1 \times first-strand synthesis buffer (Invitrogen, Carlsbad, CA) containing 1 μ g of oligo (5'-T₂₁VN-3'), 0.2 mM dNTPs, 10 mM DTT, and 200 IU of Superscript II RT (Invitrogen). The reaction mixture was incubated at 42°C for 60 min and stopped by incubation at 75°C for 15 min. Amplification of cDNA (1/20) was performed using SYBR Green PCR buffer [1 \times AmpliTaq Gold PCR buffer, 0.025 U/ μ l AmpliTaq Gold (Perkin-Elmer, Wellesley, MA), 0.2 mM dNTPs, 1 ng/ μ l 6-carboxy-X-rhodamine, 1:40,000 diluted SYBR Green dye, and 3% DMSO] and 0.1 μ M primers. The thermal cycling parameters were 95°C for 10 min, followed by 40 cycles at 95°C for 15 s and 60°C for 60 s. Before the samples were analyzed, standard curves of purified, target-specific amplicons were created. Briefly, gene-specific oligonucleotides were used to PCR amplify the gene product from a pooled sample of prepared cDNA, the concentration of the amplicons was determined by UV spectrophotometry, and a standard curve was created (100–100 million copies). The mRNA expression for each gene was determined by comparing it with its respective standard curve. This measurement was controlled for RNA quality, quantity, and RT efficiency by normalizing it to the expression level of the hypoxanthine guanine phosphoribosyl transferase (HPRT) gene. HPRT was used as a control gene because it was shown to be unaffected by any treatment used. Each primer set produced a single product, as determined by melt-curve analysis, and amplicons were of correct size, as analyzed by agarose gel electrophoresis. Statistical significance was determined by use of normalized fold changes and ANOVA.

Primers were designed using the web-based application Primer3 (http://www-genome.wi.mit.edu/cgi-bin/primer/primer3_www.cgi), biasing toward the 3'-end of the transcript to maximize the likelihood of giving a gene-specific product. The settings used in Primer3 were 125-bp amplicon, 20mer, 60°C melting temperatures, and all others as defaults. Primer sequences were analyzed by BLAST. Gene names, accession numbers, and forward and reverse primer sequences are listed in Table 1.

RESULTS

Gene expression measurements were generated after 24-h exposure to each of the five treatments, normoxia, hypoxia,

Table 3. The 62 probe sets representing the overlap between all 4 treatments

Probe Set	Fold Change				Descriptions
	HYP	COB	DFO	NICK	
1025_g_at	-10.21	-5.86	-14.71	-8.23	HSCYP450 human gene for cytochrome P(1)-450
32570_at	-6.89	-5.82	-7.28	-5.38	NAD ⁺ -dependent 15-hydroxyprostaglandin dehydrogenase (PGDH)
742_at	-4.99	-9.59	-4.44	-11.42	HUMHGFAL human mRNA for HGF activator-like protein
41772_at	-4.00	-2.18	-4.68	-2.90	monoamine oxidase A (MAOA)
38687_at	-3.45	-2.13	-3.82	-2.86	cDNA DKFZp566D193 (from clone DKFZp566D193) gb = AL050051
37322_s_at	-3.44	-4.30	-2.98	-2.53	15-hydroxy prostaglandin dehydrogenase
34297_at	-3.29	-5.82	-4.78	-3.78	putative endothelin receptor type B-like protein
34721_at	-3.07	-2.93	-3.72	-2.29	54-kDa progesterone receptor-associated immunophilin FKBP54
HUM1SGF3A	-2.90	-2.35	-2.27	-2.52	transcription factor ISGF-3
31843_at	-2.76	-3.88	-3.51	-3.30	mRNA for KIAA0832 protein, gb = AB020639
925_at	-2.63	-2.05	-6.13	-2.41	HUMIIP human gamma-interferon-inducible protein (IP-30)
32859_at	-2.59	-2.23	-2.49	-2.55	transcription factor ISGF-3 mRNA
37944_at	-2.44	-3.27	-2.79	-2.74	GTP cyclohydrolase I mRNA
40082_at	-2.32	-2.93	-2.34	-2.15	mRNA for long-chain acyl-CoA synthetase
41574_at	-2.21	-2.15	-3.79	-2.50	MEMA protein gb = Y09703
286_at	-2.20	-2.24	-3.12	-2.24	histone H2A.2 mRNA
34308_at	-2.19	-2.30	-17.01	-2.34	histone 2A-like protein (H2A/I)
35343_at	-2.02	-2.06	-3.64	-2.42	cytosolic aspartate aminotransferase
32001_s_at	2.02	3.86	5.97	2.35	subtilisin-like protein (PACE4)
41485_at	2.04	2.44	3.07	2.19	lactate dehydrogenase-A
34478_at	2.04	2.14	2.04	2.32	YPT3 mRNA gb = X79780
39366_at	2.07	5.73	5.12	2.03	protein phosphatase 1, regulatory subunit (PPP1R3C)
34378_at	2.11	3.17	3.02	2.06	adipophilin
40049_at	2.25	2.03	2.51	2.64	DAP-kinase
38970_s_at	2.35	3.02	6.14	2.68	HIV-1, Nef-associated factor 1 beta (Naf1 beta)
32210_at	2.36	5.39	13.08	2.80	phosphoglucomutase 1 (PGM1)
35780_at	2.46	3.25	7.21	2.82	<i>Homo sapiens</i> clone 23584 gb = AF035292
38010_at	2.47	13.15	10.00	2.58	E1B 19K/Bcl-2-binding protein Nip3 mRNA
39008_at	2.50	4.46	3.05	2.71	ceruloplasmin (ferroxidase)
32336_at	2.52	3.08	4.70	3.24	aldolase A
32622_at	2.59	2.07	3.84	3.01	dynammin (DNM) mRNA
1519_at	2.60	4.89	5.04	2.85	erythroblastosis virus oncogene homolog 2 (ets-2)
32538_at	2.67	2.94	3.11	3.52	transferrin
37639_at	2.83	2.34	2.69	3.04	serine protease hepsin
1826_at	2.92	2.04	8.87	3.06	human ras-related rho
33113_at	2.97	3.48	5.55	3.22	msg1-related gene 1 (mrg1)
35703_at	3.02	2.52	2.15	3.57	platelet-derived growth factor PDGF-A
34786_at	3.09	5.55	8.16	3.00	jumonji domain containing 1A
1232_s_at	3.13	10.01	26.64	2.97	human insulin-like growth factor binding protein hIGFBP1
37037_at	3.23	13.37	18.70	3.92	prolyl 4-hydroxylase
40448_at	3.44	4.51	8.06	3.61	zinc finger transcriptional regulator
34795_at	3.55	7.11	9.32	3.92	lysyl hydroxylase isoform 2 (PLOD2)
40837_at	3.94	2.47	4.15	3.77	transducin-like enhancer protein (TLE2)
36100_at	3.99	3.18	4.78	3.19	vascular endothelial growth factor
33251_at	4.04	8.73	5.48	4.43	mRNA for KIAA0779 protein gb = AB018322
41503_at	4.27	4.18	3.76	4.07	zinc fingers and homeoboxes 2
39436_at	4.40	11.61	30.92	3.48	BCL2/adenovirus E1B 19kDa-interacting protein 3a (NIX)
33143_s_at	4.44	5.41	16.85	3.31	monocarboxylate transporter (MCT3) (AKA: SLC16A3)
1953_at	4.47	2.92	4.86	3.32	vascular endothelial growth factor (VEGF)
39827_at	4.72	4.39	4.70	6.80	DNA-damage-inducible transcript 4 (DDIT4)
36386_at	4.75	10.81	14.86	3.88	pyruvate dehydrogenase kinase isoenzyme 1 (PDK1)
40790_at	4.88	4.03	8.02	4.21	DEC1
36101_s_at	5.04	3.60	7.25	4.13	vascular endothelial growth factor
38545_at	5.16	2.48	12.07	4.03	testicular inhibin beta-B-subunit
40926_at	5.79	12.05	25.49	6.74	creatine transporter (SLC6A8)
38125_at	6.30	10.63	22.79	7.93	beta-migrating plasminogen activator inhibitor I
34777_at	6.77	33.13	39.45	3.87	adrenomedullin precursor
40309_at	8.05	39.37	39.90	5.70	carbonic anhydrases (MaTu MN)
1591_s_at	11.93	2.19	8.58	8.53	insulin-like growth factor II
36782_s_at	13.92	2.28	10.26	13.20	insulin-like growth factor II
36933_at	79.94	127.74	241.04	61.55	RTP (N-myc downstream regulated gene 1)
2079_s_at	255.59	27.64	140.03	202.67	insulin-like growth factor (IGF-II)

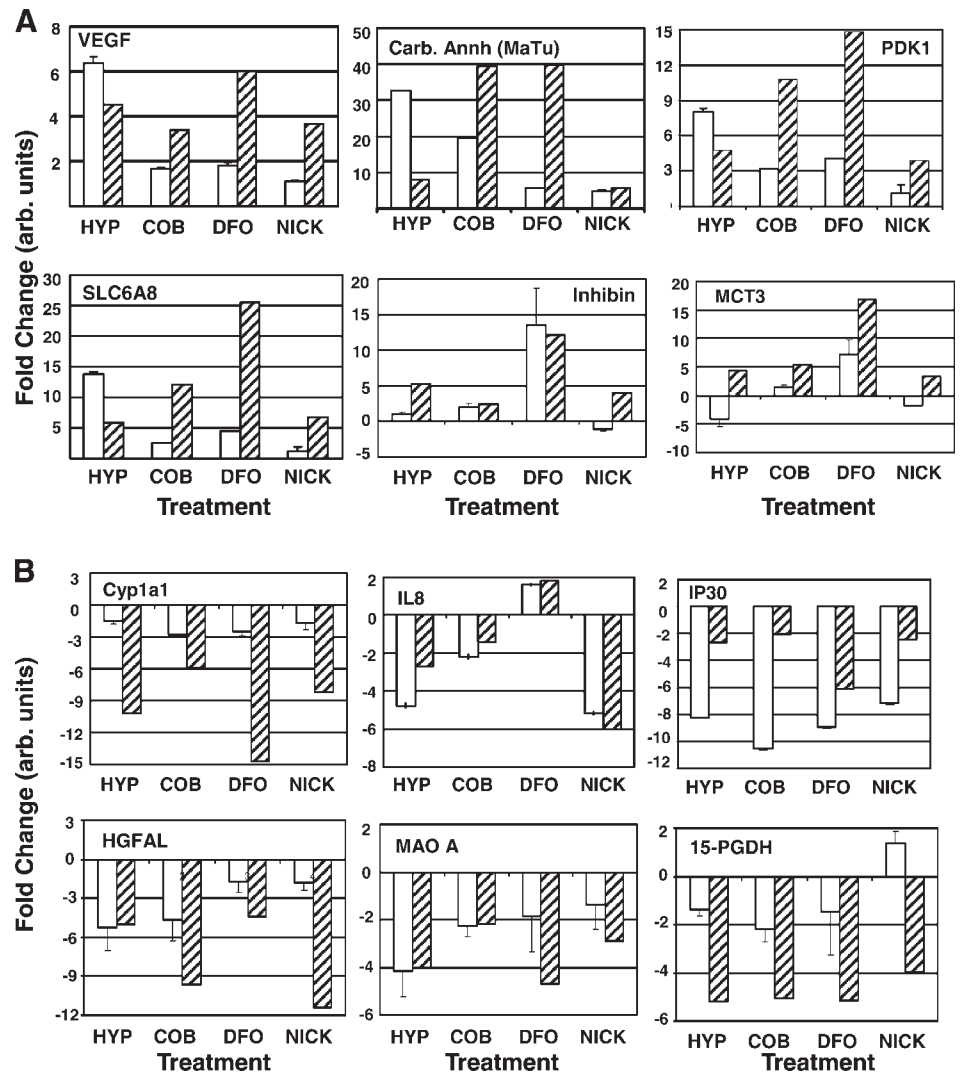


Fig. 2. Quantitative RT-PCR (qRT-PCR) verification of 12 genes. The expression pattern for 6 upregulated genes (A) and 6 downregulated genes (B) was verified by qRT-PCR using SYBR Green as a marker. SYBR Green data (open bars) is directly compared with the microarray data (hatched bars). Gene names are listed at the top of each graph. HYP, hypoxia (1% O₂); COB, cobalt (100 μM CoCl₂); DFO, 100 μM deferoxamine; NICK, nickel (100 μM NiCl₂).

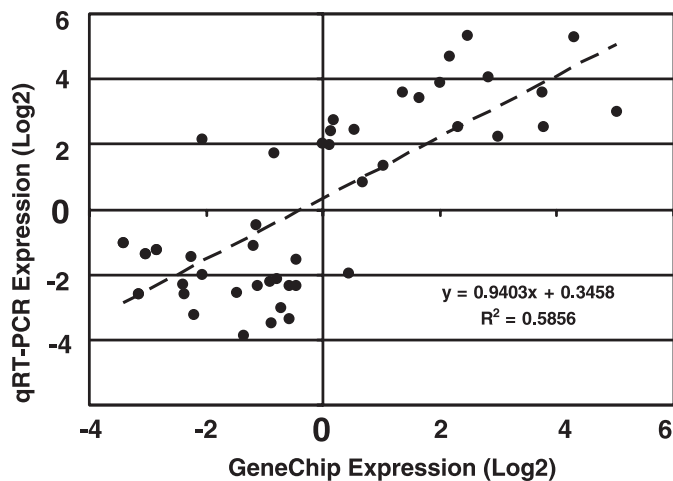


Fig. 3. Analytical comparison of qRT-PCR and microarray data. Fold-change values from qRT-PCR and microarray results were log₂ transformed and plotted on a linear graph. Linear regression was performed, and equation of the line and R² values are listed.

cobalt, nickel, and DFO, in Hep3b cells. To examine the global relatedness of each of these stimuli, we performed hierarchal clustering on the entire data set. These results indicated that there is considerable similarity between the four stimuli (data not shown). To directly compare the effects of these treatments on the complete data set, an ANOVA was performed. The results showed that >38% (3,404/12,626 probe sets) were significantly influenced ($P < 0.05$) by treatment. These results suggest that hypoxia and hypoxia mimics have profound effects on cellular homeostasis and that there is considerable similarity between the four hypoxia treatments.

A direct comparison of each treatment was also performed to identify subsets of genes that were shared and those that were unique among treatment groups. Genes with significantly altered expression ($P < 0.05$ and >2-fold change) were compared. At these significance levels, hypoxia (1% O₂) influenced 451 different probe sets. These sets of responsive genes included well-known hypoxia-regulated genes including GAPDH, VEGF, insulin-like growth factor II (IGF-II), carbonic anhydrase, and plasminogen activator inhibitor I (PAI-I) (19, 27) (Table 2). This list of hypoxia-responsive genes also included several genes that had not previously been demonstrated to be modu-

Table 4. Top 20 up- and downregulated genes specific to HYP (1% O₂)

Probe Set	Fold Change				Descriptions
	HYP	COB	DFO	NICK	
38680_at	-4.43	-1.37	-1.63	-2.05	Alu repeats in the small nuclear ribonucleoprotein E
36636_at	-4.00	1.03	1.09	-1.91	omithine aminotransferase
36671_at	-3.43	-1.34	-1.52	-1.78	asparagine synthetase
40629_at	-3.05	1.15	-1.61	-1.29	GPI-H mRNA
40074_at	-3.05	-1.05	-1.31	-1.99	NAD-dependent methylene THF-DH cyclohydrolase
36604_at	-3.04	1.02	-1.66	-1.92	ubiquitin-conjugating enzyme E2
32777_at	-3.00	1.14	-1.80	-1.90	CHD5 protein
39983_at	-2.80	-1.88	-1.92	-2.76	FKBP-associated protein FAP48
38029_at	-2.80	-1.29	-1.07	-1.77	glycoprotein 4F2
41536_at	-2.75	1.27	-1.21	-1.77	AL022726 clone 625H18
34366_g_at	-2.75	1.10	-1.33	-1.76	cyclophilin-33B (CYP-33)
36857_at	-2.70	-1.30	-1.69	-1.90	DNA repair exonuclease (REC1)
38983_at	-2.69	-1.11	-1.85	-1.73	AI223047 cDNA
33434_at	-2.62	1.46	-1.87	-1.52	Bet1p homolog (hbet1)
40250_at	-2.60	-1.46	-1.97	-2.51	Rev interacting protein Rip-1
402_s_at	-2.60	1.56	-1.08	-1.54	ICAM-3 mRNA
262_at	-2.58	-1.10	-1.42	-1.57	S-adenosylmethionine decarboxylase
40568_at	-2.56	-1.11	-1.50	-1.92	vacuolar H ⁺ -ATPase
34356_at	-2.54	1.23	-1.57	-1.80	polymerase II complex component SRB7
38725_s_at	-2.50	-1.81	-1.62	-1.86	N36295 cDNA
37657_at	2.01	-1.03	1.86	1.50	PALM gene
38586_at	2.03	-1.67	1.10	1.14	fatty acid binding protein (FABP)
41657_at	2.03	1.33	1.23	1.54	serine threonine kinase 11
40186_at	2.04	1.54	1.15	1.83	MAP kinase phosphatase 4
1443_at	2.04	1.50	1.42	2.78	HSMAPKP4 MAP kinase phosphatase 4
41366_at	2.12	-1.04	-1.40	1.96	mRNA for KIAA1002
32583_at	2.13	1.51	1.81	1.70	c-jun proto oncogene (JUN)
38757_at	2.14	-1.14	1.42	1.87	PDGF associated protein
835_at	2.14	-1.89	1.71	1.87	PDGF associated protein
41061_at	2.17	-1.14	-1.15	1.61	huntingtin interacting protein 1
34303_at	2.21	1.23	1.75	1.86	AL049949 mRNA
40960_at	2.28	-1.02	1.75	1.79	beta-1,4-galactosyltransferase
HSAC07	2.31	-1.00	1.01	1.09	beta-actin
37880_at	2.33	1.25	1.33	1.67	L-alanine-glyoxylate aminotransferase
39385_at	2.41	-1.15	1.48	1.79	aminopeptidase N/CD13
38295_at	2.47	-1.00	1.53	1.87	PBX2 mRNA
hum_alu_at	2.55	-1.18	1.69	1.68	Alu-Sq subfamily
37884_f_at	2.66	4.75	2.50	1.81	AI375033 cDNA
41872_at	2.69	1.32	-1.37	1.72	nonsyndromic hearing impairment protein (DFNA5)
34610_at	8.57	-1.01	1.65	3.13	guanine nucleotide binding protein

lated by low O₂ tension. For example, pyruvate dehydrogenase kinase-1 (PDK1) and the creatine transporter SLC6A8 were upregulated 4.7- and 5.7-fold, respectively. In addition, the NAD⁺-dependent 15-hydroxyprostaglandin dehydrogenase (15-PDGH) and prohibitin genes were significantly downregulated after hypoxia exposure. These results confirm the appropriateness of our data analysis and suggest that a more complete set of hypoxia-responsive genes were identified.

The other three treatments, cobalt, DFO, and nickel, also had profound physiological effects on the cells. Cobalt exposure (100 μM, 24 h) led to the significant change ($P < 0.05$ and >2 -fold) in transcription of 303 probe sets (Fig. 1). Of these 303 probe sets, 85 (28%) overlapped with the hypoxia-responsive subset. Nickel exposure altered the expression of a similar number of genes as cobalt (325 probe sets); however, a higher percentage overlapped with the hypoxia subset (65.2%, 212/325 probe sets) (Fig. 1). DFO treatment led to altered expression of a much larger number of probe sets under these conditions (100 μM, 24 h). DFO exposure changed the expression of 1,068 different probe sets, and 23.3% (249/1,068 probe sets) were shared with the hypoxia subset (Fig. 1). These data

suggest that there is a core set of genes that are responsive to hypoxia and hypoxia mimics, but a larger population may be unique to each treatment.

To more thoroughly understand this core set of genes, a comprehensive analysis of those genes that were shared between all four treatment groups was performed. This analysis led to the identification of a core set of 62 probe sets, representing 55 different genes (Table 3). This list contains a large group of previously characterized hypoxia-responsive genes, including IGF-II, *N*-myc downstream regulated (also known as NDR1, RTP, and CAP43), PAI-I, VEGF, and several glycolytic enzyme genes. The list also contains several genes that had not been characterized as hypoxia responsive. These include PDK1, PDGH, MAOA, inhibin, and SLC6A8.

To verify the expression of some of the novel hypoxia-regulated genes, as well as some of the conventional hypoxia targets, quantitative RT-PCR (qRT-PCR) was performed. The genes verified included VEGF and carbonic anhydrase as controls for the hypoxia treatments. These genes are known hypoxia genes, and qRT-PCR and microarray data were in good agreement. In addition, four other genes (PDK1,

Table 5. Top 20 up- and downregulated genes specific to CoCl₂ (100 μM)

Probe Set	Fold Change				Descriptions
	HYP	COB	DFO	NICK	
41320_s_at	1.56	-3.76	-1.57	-1.07	transcriptional repressor (GCF2)
2017_s_at	1.90	-3.75	1.13	1.29	human cyclin D (cyclin D1)
37637_at	-1.20	-3.73	-1.52	-1.34	RGP3 mRNA
867_s_at	1.31	-3.58	1.36	1.26	thrombospondin-1
36638_at	-1.27	-3.47	1.11	-1.74	connective tissue growth factor
1143_s_at	-1.26	-3.41	-1.89	-1.68	fibroblast growth factor receptor K-Sam
38418_at	-1.07	-3.10	-1.53	-1.23	PRAD1 mRNA for cyclin
33436_at	-1.42	-2.95	-1.12	-1.26	SOX9 mRNA
34517_at	1.31	-2.90	-1.20	1.18	HMG-CoA-synthase
2020_at	-1.31	-2.86	-1.86	-1.20	bcl-1 mRNA
33389_at	-1.24	-2.75	-1.76	-1.26	cytochrome P450 (CYP51)
38686_at	-1.42	-2.64	-1.26	-1.27	vacuolar proton ATPase
31521_f_at	-1.64	-2.60	-2.00	-1.51	H4/e gene for H4 histone
1787_at	-1.08	-2.60	-1.30	-1.71	Cdk-inhibitor p57KIP2
34213_at	-1.17	-2.57	1.20	-1.58	mRNA for KIAA0869 protein
404_at	-1.17	-2.54	-1.92	-1.32	interleukin 4 receptor
1970_s_at	-1.09	-2.48	-1.85	-1.34	FGFR2 mRNA
866_at	-1.24	-2.43	-1.70	-1.23	thrombospondin-1
33369_at	1.05	-2.42	-1.95	1.44	AI535653 cDNA
40841_at	-1.04	-2.37	1.12	-1.33	TACC1 (TACC1) mRNA
35284_f_at	-1.63	2.83	-1.72	-1.78	W28620 cDNA
37002_at	1.33	2.91	1.12	1.32	biliverdin-IXbeta reductase I
38825_at	1.06	2.95	1.02	-1.06	fibrinogen alpha chain gene
1962_at	1.66	2.95	1.04	1.74	liver arginase
40838_at	1.56	3.11	1.46	1.31	mRNA for KIAA0530 protein
35214_at	-1.57	3.32	-1.21	1.73	UDP-glucose dehydrogenase (UGDH)
38876_at	-1.29	3.70	-1.06	1.34	AL080091 cDNA
31850_at	-1.41	3.89	1.26	1.27	gamma-glutamylcysteine synthetase
35724_at	-1.23	4.11	-1.46	1.50	Plrin, isolate 1
32664_at	-1.16	4.62	2.07	1.56	RNase 4
35686_s_at	-1.42	4.82	2.03	-1.34	MTCP1 gene
39365_i_at	1.19	4.95	1.70	1.12	protein phosphatase 1 (PPP1R5)
35194_at	1.12	5.05	1.00	1.05	glutathione peroxidase-like protein
748_s_at	1.20	5.79	3.44	1.35	Mxi1 protein
34342_s_at	1.16	6.93	1.01	1.07	osteopontin mRNA
39120_at	-1.32	9.41	-1.32	-1.49	AA224832 cDNA
37399_at	1.11	9.57	1.00	1.03	mRNA for KIAA0119 gene
38379_at	1.16	11.24	1.02	1.07	NMB mRNA
32805_at	-1.30	64.02	-1.95	-1.60	hepatic dihydrodiol dehydrogenase
32392_s_at	1.13	80.74	1.01	1.19	bilirubin UDP-glucuronosyltransferase isozyme 2

SLC6A8, inhibin, and MCT3) that were upregulated in all four treatments and had not been characterized as hypoxia regulated were also verified. Each of the four treatments led to the upregulation of the PDK1 and SLC6A8 genes in the microarray and qRT-PCR analysis (Fig. 2A). In addition, the qRT-PCR expression pattern of inhibin correlated with the microarray data in three of the four treatments, while MCT3 was only verified in the DFO treatment group (Fig. 2A).

There were also several downregulated genes that were verified by qRT-PCR (Fig. 2B). Cyp1a1 was downregulated in all four treatments in both the microarray and qRT-PCR experiments, and this is in good agreement with previously published reports (7, 8). IL-8 was downregulated in three of the four treatments on the microarray, and this pattern was verified in the qRT-PCR results. Finally, four genes (HG-FAL, IP30, MAOA, and 15-PGDH) were downregulated in all four treatments on the microarray, and this was confirmed on the qRT-PCR, with one exception. Nickel induced a slight upregulation in the 15-PGDH gene in the qRT-PCR (Fig. 2B).

A direct comparison of the microarray and qRT-PCR data was performed by compiling all of the values for all 12 genes

under all 4 conditions and plotting them on a log₂ chart (Fig. 3). The graph was further analyzed by linear regression and displayed a slope of 0.94 and an R² value of 0.58. These results validate the microarray data analysis and suggest that there is very good correlation between the two assays.

The results suggest that there is considerable overlap between the various treatments; however, there is also a large subset of genes that were altered in a treatment-specific manner. The expression of these genes passed significance and fold-change cutoffs in only one treatment. For example, there were 121 probe sets whose expression was altered ($P < 0.05$ and >2 -fold) after hypoxia treatment that were not significantly changed in the other three treatment groups (Fig. 1, Table 4). This subset included probe sets for the guanine nucleotide-binding protein, *c-jun*, MAP kinase phosphatase-4, ubiquitin-conjugating enzyme E2, and asparagine synthetase (Table 4). The role these genes play in the cellular response to hypoxia is currently being investigated.

There were also 92, 676, and 49 probes sets that were specific to cobalt, DFO, and nickel, respectively (Fig. 1). These subsets include growth factors (e.g., connective tissue growth factor, amphiregulin, and transforming growth factor-β), struc-

Table 6. Top 20 up- and downregulated genes specific to DFO (100 μ M)

Probe Set	Fold Change				Descriptions
	HYP	COB	DFO	NICK	
38519_at	-1.40	-1.92	-27.06	-1.18	famesol receptor HRR-1
527_at	-1.89	-1.64	-10.50	-1.33	centromere protein-A (CENP-A)
1647_at	-1.21	-1.81	-7.84	-1.22	RasGAP-related protein (IQGAP2)
40238_at	-1.56	-1.33	-7.31	-2.03	AI674208 cDNA
1599_at	-1.91	-1.62	-6.45	-1.76	protein tyrosine phosphatase (CIP2)
34851_at	-1.56	-1.12	-6.30	-1.29	serine/threonine kinase (BTAK)
37173_at	-1.96	-2.12	-6.22	-1.73	CENP-E mRNA
37649_at	-1.98	-1.22	-6.03	-1.61	hydroxymethylbilane synthase gene
38099_r_at	-1.30	-1.67	-5.99	-1.33	acyl-CoA synthetase 4 (ACS4)
38717_at	1.61	-1.27	-5.91	1.77	AL050159 cDNA
40508_at	-2.00	1.35	-5.77	-1.53	glutathione S-transferase A4-4 (GSTA4)
33701_at	-1.63	-1.83	-5.68	-1.51	phenylalanine hydroxylase (PAH)
41211_at	-1.29	-1.19	-5.64	-1.03	mRNA for KIAA0765 protein
34852_g_at	-1.43	-1.10	-5.60	-1.26	serine/threonine kinase (BTAK)
1945_at	-1.75	-1.48	-5.56	-1.63	cyclin B
41352_at	1.19	1.26	-5.51	1.58	beta-galactoside alpha-2,6-sialyltransferase
37302_at	-1.76	-1.86	-5.48	-1.75	mitosin mRNA
38824_at	-1.86	1.49	-5.41	-1.38	Tat-interacting protein TIP30
903_at	-1.12	-1.93	-5.31	-1.54	phosphatase 2A B56-alpha (PP2A)
37235_g_at	-1.78	-1.81	-5.24	-1.40	alpha-2-thiol proteinase inhibitor
39279_at	1.07	-1.03	6.44	1.02	transforming growth factor-beta
35174_i_at	1.30	1.13	6.61	1.45	elongation factor 1 alpha-2
38790_at	1.03	1.94	6.69	1.29	p53/HEH epoxide hydrolase (EPHX)
38457_at	1.49	1.02	6.70	1.09	troponin I fast-twitch isoform mRNA
36543_at	1.56	-1.28	6.86	1.07	coagulation factor III
1690_at	1.62	1.58	7.18	1.15	TGF-beta superfamily protein
1733_at	1.16	1.01	7.66	1.08	transforming growth factor-beta
39302_at	1.04	2.91	8.02	-1.10	desmocollins type 2a and 2b
35617_at	1.63	1.28	8.21	1.73	BMK1 alpha kinase
37111_g_at	1.35	1.48	8.51	1.35	fructose-6-phosphate,2-kinase/fructose-2, 6-bisphosphatase
32899_s_at	1.32	1.13	9.05	1.11	orphan hormone nuclear receptor RORalpha1
1113_at	-1.03	-1.39	10.03	-1.52	bone morphogenetic protein 2A
1915_s_at	1.28	1.05	10.25	1.06	cellular oncogene c-fos
287_at	1.02	-1.05	11.22	-1.09	activating transcription factor 3
40367_at	1.09	-1.23	11.28	-1.10	morphogenetic protein 2A
41038_at	1.47	3.58	11.46	-1.49	neutrophil oxidase factor (p67-phox)
39248_at	-1.26	1.53	11.71	1.22	N74607cDNA
34661_at	-1.03	-1.30	17.11	1.68	mRNA for KIAA0350
33127_at	1.20	1.71	21.51	1.09	lysyl oxidase-related protein (WS9-14)
1916_s_at	1.37	1.12	29.73	1.12	cellular oncogene c-fos

tural proteins (e.g., desmocollin, spectrin, and adducin), and genes for several important enzymes (e.g., glutathione-S-transferase, hepatic dihydrodiol dehydrogenase, and S-adenosylmethionine synthetase). In addition, each treatment altered the expression of various critical transcription factors and cell cycle regulators. For example, cobalt exposure led to the decreased expression of cyclin D1 (Table 5). DFO had the largest unique set of genes, and it contained the transcription factors *c-fos*, activating transcription factor-3, and the farnesol receptor HRR-1 (Table 6). Nickel altered the expression of the genes for the transcription factors E2A and SL1 (Table 7). These results suggest that each of these treatments has a different functional consequence on cellular homeostasis, making it unique from hypoxia exposure.

DISCUSSION

Several dozen genes responded to both cellular hypoxia and its mimics. These genes included known hypoxia-regulated genes, such as IGF-II, VEGF, and carbonic anhydrase, but also many previously uncharacterized genes that were altered by all four treatments. Several genes were involved in the processes

of adaptation and cell death, indicating a delicate balance between these processes under hypoxic stress. Adaptive genes included the previously known glycolytic enzymes and carbonic anhydrase but also the creatine transporter SLC6A8, through which creatine may function to regulate the ATP supply within the cell (25). Another gene induced by hypoxia and its mimics, PDK1, is responsible for inactivating the pyruvate dehydrogenase (PDH) complex and thus regulating the amount of glucose that is ultimately converted to acetyl-CoA. The upregulation of PDK1 and subsequent inactivation of the PDH complex may act to divert pyruvate to other metabolic pathways to cope with the hypoxic environment.

Conversely, apoptotic or cell death-promoting genes and cell proliferation inhibitors were also found to be regulated by all four hypoxic stimuli. These include the known hypoxic targets BCL2/adenovirus E1B 19-kDa-interacting protein-3a (NIX), which can promote apoptosis or necrosis depending on cell type and circumstances, and DEC1 (deleted in esophageal cancers 1), an anti-proliferation and putative tumor suppressor gene (13, 22, 30, 34). This list also included RTP801 (also known as DDIT4 and *N-myc* downstream-regulated gene 1).

Table 7. Top 20 up- and downregulated genes specific to NiCl₂ (100 μM)

Probe Set	Fold Change				Descriptions
	HYP	COB	DFO	NICK	
34898_at	-2.16	-1.75	1.75	-2.92	amphiregulin (AR)
37701_at	-1.97	-1.61	-1.34	-2.88	helix-loop-helix basic phosphoprotein (GDS8)
35803_at	-2.91	-1.62	1.25	-2.61	RhoE = 26 kda GTPase homolog
41662_at	-4.46	1.10	1.00	-2.49	AL050272 cDNA
39351_at	-1.85	-1.98	-1.29	-2.46	transmembrane protein (CD59)
36191_at	-2.92	-1.32	-1.99	-2.45	mitochondrial transcription factor 1
36079_at	-2.63	-1.96	-1.49	-2.33	Pig3 (PIG3)
38678_at	-1.62	-1.12	-1.78	-2.28	AA733050 cDNA
32088_at	-1.78	1.04	-1.40	-2.28	basic-leucine zipper nuclear factor (JEM-1)
35842_at	-1.75	-1.19	-1.10	-2.20	AL049265 cDNA
40269_at	-2.08	-1.35	-2.00	-2.13	hPrp 18 mRNA
35006_at	-1.47	-1.51	-1.61	-2.11	transcription factor SL1
32102_at	-1.56	-1.21	-1.04	-2.11	AB018273 mRNA
39506_at	-1.37	1.05	-1.04	-2.09	AA933984 cDNA
39224_at	-1.24	-1.24	-1.33	-2.08	AB011152 mRNA
1536_at	-1.19	1.09	-1.34	-2.07	Cdc6-related protein (HsCDC6)
1119_at	-2.07	-1.24	-1.43	-2.06	human replication protein A
38381_at	-1.49	-1.55	-1.63	-2.06	syntaxin 3
39533_at	-1.81	1.14	1.14	-2.05	D87432 mRNA
339_at	-1.96	-1.15	1.49	-2.05	caveolin-2
31431_at	1.71	1.19	1.24	2.06	IgG Fc receptor
1047_s_at	1.41	1.05	1.09	2.09	hepatocyte growth factor-like protein gene
41725_at	1.78	1.17	1.81	2.09	casein kinase I gamma 2
36784_at	2.40	-1.03	1.96	2.11	growth hormone and chorionic somatomammotropin
38406_t_at	1.96	1.12	1.19	2.12	AI207842 cDNA
39358_at	1.61	1.28	1.54	2.12	silencing mediator of retinoid and thyroid hormone action
35154_at	1.63	1.57	1.55	2.13	W68046 cDNA
33630_s_at	1.34	1.01	-1.09	2.13	beta III spectrin (SPTBN2)
121B_at	1.76	1.24	1.42	2.13	v-erbA related ear-2
32146_s_at	2.01	1.58	2.24	2.18	alpha adducin
1374_g_at	1.62	1.82	1.29	2.22	transcription factor (E2A)
39372_at	1.88	-1.50	-1.14	2.28	W26480 cDNA
38789_at	1.48	1.80	1.13	2.29	transketolase
40850_at	1.96	1.67	1.68	2.29	FK-506 binding protein homologue (FKBP38)
446_at	1.85	-1.09	1.93	2.37	casein kinase I gamma 2
32800_at	1.88	1.04	1.29	2.53	retinoid X receptor alpha mRNA
1373_at	1.84	1.30	1.70	2.57	transcription factor (E2A)
39560_at	1.55	1.64	1.00	2.73	H10776 cDNA
32571_at	1.10	-1.08	-1.92	2.73	S-adenosylmethionine synthetase
35547_at	5.15	1.19	3.27	6.25	monocarboxylate transporter 2 (hMCT2)

RTP801 (upregulated 80-fold by hypoxia) was previously described as a hypoxia-inducible gene that plays a complex role in cellular viability (28). Under certain conditions, it can act in a protective manner; however, under most standard conditions, overexpression of RTP801 leads to cell death. Collectively, these results indicate that hypoxia and its mimics induce a complex interplay between adaptive and proapoptotic responses that ultimately dictates cell survival.

Several genes that were identified and verified suggest a complex cellular response to hypoxia. There is an initial upregulation of the glycolytic enzymes as a way of coping with an inability to produce ATP through oxidative phosphorylation. This upregulation may also be important to the maintenance of critical cellular metabolites (11). This adaptive response is supported by other cellular processes, such as creatine transport (SLC6A8), which may allow the cell to survive in the hypoxic environment. The decrease in Cyp11a1 may be an attempt to control oxygen usage in side reactions or partial limits due to ARNT availability. HGFAL is a serine protease involved in cellular adhesion and is downregulated in all four treatments. Another downregulated target is inhibin-β. When bound to inhibin-α, the dimer is

capable of inhibiting follicle-stimulating hormone and a putative tumor suppressor. Finally, IP30 (also known as γ-interferon-inducible protein; GILT) is a lysosomal thiol reductase involved in disulfide bond reduction at low pH and is downregulated under all four conditions tested (20). The role these proteins play in the adaptive or cell death response to hypoxia is unknown and under further investigation.

Current genomic technology has begun to unravel the various signaling networks that are influenced, both directly and indirectly, by hypoxia. Several recent publications from our laboratory and others have begun to characterize a complete list of "hypoxia" target genes (24, 29, 32). A direct comparison between global expression data is difficult when different platforms and cell types have been employed; however, comparison of the present study and recently published reports suggest that hypoxia and hypoxia mimics (i.e., nickel, cobalt, and DFO) alter the expression of a core set of genes, including glycolytic enzymes, apoptotic genes, and several hydroxylases. The hydroxylases include EGLN1 (also known as PHD2, HPH2), an enzyme responsible for regulating HIF1α stability. More importantly, the differences seen in these various studies

suggest that cell type and treatment paradigms can drastically influence the list of hypoxia genes identified in these genomic screens.

These differences can be highlighted when the genes that were modulated by all four treatments of this study (Table 3) are compared with genes that were influenced by hypoxia and cobalt in mouse fibroblast (Table 2, Ref. 32). There was only limited overlap between these two studies, and most of these were known hypoxia-regulated genes (e.g., lactate dehydrogenase, prolyl-4-hydroxylase, aldolase, and NIX). When this comparison is extended to a direct comparison of 24-h hypoxia treatments in Hep3B cells (Table 4 and Supplemental Data; available at the *Physiological Genomics* web site)¹ and mouse fibroblasts (Supplemental Table SD, Ref. 32), ~18% of the clones are present in both lists (51 of 287 clones). Again, most of these clones were known hypoxia target genes, including the glycolytic enzymes and the apoptotic gene BNIP3 (31, 32). The clones included in this overlap, however, also included some novel targets, such as 17- β -hydroxysteroid dehydrogenase. The 11- β -hydroxysteroid dehydrogenase gene has previously been shown to be a target of hypoxia-mediated downregulation, and the addition of this family member may suggest a global downregulation of steroid synthesis under hypoxic conditions (14). In addition, we could detect no significant change in expression of ataxia telangiectasia mutated (ATM) or focal adhesion kinase (FAK) after exposure to any of the four treatments used, even though these genes were expressed in this cell type. This is in contrast to nickel-treated mouse fibroblasts, where a significant increase in ATM and FAK was observed (24). Given the similarity in platforms, these differences are probably due to cell-specific signaling.

The most similar genomic screen to the one reported here was performed in HepG2 cells and utilized the same platform (29). When the complete list of hypoxia-responsive genes (Supplemental Data) was compared with the HepG2 study, there was ~10% overlap (47/452) (29). This overlap was weighted toward upregulated genes (36 of 47 probe sets), even though a higher proportion of genes in our list (Supplemental Data) were downregulated (314 of 452). The overlap included genes such as IP30, several heat shock proteins, and classic hypoxia-regulated genes, but several of the genes verified in this study (e.g., HGFAL and IL-8) were not differentially expressed in the HepG2 cells after hypoxia exposure. Finally, in a recent publication, serial analysis of gene expression (SAGE) was used to identify genes whose levels were altered by loss of the VHL protein (18). VHL plays an essential role in regulating hypoxia signaling by recognizing the hydroxylated form of the HIF and recruiting the ubiquitination machinery necessary for its degradation. Therefore, we hypothesized significant overlap between our results and those derived from the SAGE experiments (18). Indeed, there was extensive overlap, including genes such as plasminogen activator inhibitor, BNIP3a, and IP30. These results suggest that there is a core set of hypoxia-inducible genes in all cell types and that each also harbors the ability to mount specific responses to low oxygen availability.

Adaptive responses to hypoxia involve a complex network of signaling pathways and are necessary for cell and organismal survival. Current studies of hypoxia rely heavily on mimics such as cobalt chloride and DFO, which presumably function by inhibiting the iron-dependent hydroxylases that regulate HIF1 α stability. However, the possibility that cobalt and DFO have other activities that may complicate analysis of these experiments has not been fully addressed. Our results indicate that the overlap between these mimics and hypoxia is limited and suggest caution in their use. In addition, we show that many genes are induced by all four stimuli including glycolytic enzymes and other survival genes (i.e., SLC6A8), hydroxylases, and apoptotic genes. A detailed mechanistic understanding of how cells respond to low oxygen, cobalt, and DFO, including their transcriptional programs, will ultimately be required for a more complete understanding of hypoxia-mediated signaling and how it relates to critical processes of development and cancer.

ACKNOWLEDGMENTS

We thank Jennifer Villasenor and Mimmi Hayakawa for technical assistance, John Walker for help with data processing and analysis, and Dr. Christopher Bradfield for support during the initial phases of these experiments.

REFERENCES

- Berra E, Benizri E, Ginouvès A, Volmat V, Roux D, and Pouyssegur J. HIF prolyl-hydroxylase 2 is the key oxygen sensor setting low steady-state levels of HIF-1 α in normoxia. *EMBO J* 22: 4082–4090, 2003.
- Blanchard KL, Acquaviva AM, Galson DL, and Bunn HF. Hypoxic induction of the human erythropoietin gene: cooperation between the promoter and enhancer, each of which contains steroid receptor response elements. *Mol Cell Biol* 12: 5373–5385, 1992.
- Bruick RK and McKnight SL. A conserved family of prolyl-4-hydroxylases that modify HIF. *Science* 294: 1337–1340, 2001.
- Bunn HF and Poyton RO. Oxygen sensing and molecular adaptation to hypoxia. *Physiol Rev* 76: 839–885, 1996.
- Cioffi CL, Liu XQ, Kosinski PA, Garay M, and Bowen BR. Differential regulation of HIF-1 α prolyl-4-hydroxylase genes by hypoxia in human cardiovascular cells. *Biochem Biophys Res Commun* 303: 947–953, 2003.
- Epstein AC, Gleadle JM, McNeill LA, Hewitson KS, O'Rourke J, Mole DR, Mukherji M, Metzén E, Wilson MI, Dhanda A, Tian YM, Masson N, Hamilton DL, Jaakkola P, Barstead R, Hodgkin J, Maxwell PH, Pugh CW, Schofield CJ, and Ratcliffe PJ. *C. elegans* EGL-9 and mammalian homologs define a family of dioxygenases that regulate HIF by prolyl hydroxylation. *Cell* 107: 43–54, 2001.
- Fradette C, Bleau AM, Pichette V, Chauréat N, and Du Souich P. Hypoxia-induced down-regulation of CYP1A1/1A2 and up-regulation of CYP3A6 involves serum mediators. *Br J Pharmacol* 137: 881–891, 2002.
- Fradette C and Du Souich P. Effect of hypoxia on cytochrome P450 activity and expression. *Curr Drug Metab* 5: 257–271, 2004.
- Gentleman RC, Carey VJ, Bates DM, Bolstad B, Dettling M, Dudoit S, Ellis B, Gautier L, Ge Y, Gentry J, Hornik K, Hothorn T, Huber W, Iacus S, Irizarry R, Leisch F, Li C, Maechler M, Rossini AJ, Sawitzki G, Smyth G, Tierney L, Yang JY, and Zhang J. Bioconductor: open software development for computational biology and bioinformatics. *Genome Biol* 5: R80, 2004.
- Gleadle JM and Ratcliffe PJ. Hypoxia and the regulation of gene expression. *Mol Med Today* 4: 122–129, 1998.
- Griffiths JR, McSheehy PM, Robinson SP, Troy H, Chung YL, Leek RD, Williams KJ, Stratford IJ, Harris AL, and Stubbs M. Metabolic changes detected by in vivo magnetic resonance studies of HEP-1 wild-type tumors and tumors deficient in hypoxia-inducible factor-1 β (HIF-1 β): evidence of an anabolic role for the HIF-1 pathway. *Cancer Res* 62: 688–695, 2002.
- Gu YZ, Hogenesch J, and Bradfield C. The PAS superfamily: sensors of environmental and developmental signals. *Annu Rev Pharmacol Toxicol* 40: 519–561, 2000.

¹ The Supplemental Material for this article is available online at <http://physiolgenomics.physiology.org/cgi/content/full/00045.2004/DC1>.

13. Guo K, Searfoss G, Krolkowski D, Pagnoni M, Franks C, Clark K, Yu KT, Jaye M, and Ivashchenko Y. Hypoxia induces the expression of the pro-apoptotic gene BNIP3. *Cell Death Differ* 8: 367–376, 2001.
14. Heiniger CD, Kostadinova RM, Rochat MK, Serra A, Ferrari P, Dick B, Frey BM, and Frey FJ. Hypoxia causes down-regulation of 11 β -hydroxysteroid dehydrogenase type 2 by induction of Egr-1. *FASEB J* 17: 917–919, 2003.
15. Ihaka R and Gentleman R. R: a language for data analysis and graphics. *J Comp Graph Stats* 5: 299–314, 1996.
16. Iyer NV, Kotch LE, Agani F, Leung SW, Laughner E, Wenger RH, Gassmann M, Gearhart JD, Lawler AM, Yu AY, and Semenza GL. Cellular and developmental control of O₂ homeostasis by hypoxia-inducible factor 1 α . *Genes Dev* 12: 149–162, 1998.
17. Jaakkola P, Mole DR, Tian YM, Wilson MI, Gielbert J, Gaskell SJ, Kriegsheim A, Hebestreit HF, Mukherji M, Schofield CJ, Maxwell PH, Pugh CW, and Ratcliffe PJ. Targeting of HIF- α to the von Hippel-Lindau ubiquitylation complex by O₂-regulated prolyl hydroxylation. *Science* 292: 468–472, 2001.
18. Jiang Y, Zhang W, Kondo K, Klco JM, St Martin TB, Dufault MR, Madden SL, Kaelin WG Jr, and Nacht M. Gene expression profiling in a renal cell carcinoma cell line: dissecting VHL and hypoxia-dependent pathways. *Mol Cancer Res* 1: 453–462, 2003.
19. Levy AP, Levy NS, Wegner S, and Goldberg MA. Transcriptional regulation of the rat vascular endothelial growth factor gene by hypoxia. *J Biol Chem* 270: 13333–13340, 1995.
20. Luster AD, Weinshank RL, Feinman R, and Ravetch JV. Molecular and biochemical characterization of a novel γ -interferon-inducible protein. *J Biol Chem* 263: 12036–12043, 1988.
21. Metzen E, Berchner-Pfannschmidt U, Stengel P, Marxsen JH, Stolze I, Klinger M, Huang WQ, Wotzlav C, Hellwig-Burgel T, Jelkmann W, Acker H, and Fandrey J. Intracellular localisation of human HIF-1 α hydroxylases: implications for oxygen sensing. *J Cell Sci* 116: 1319–1326, 2003.
22. Nishiwaki T, Daigo Y, Kawasoe T, and Nakamura Y. Isolation and mutational analysis of a novel human cDNA, DEC1 (deleted in esophageal cancer 1), derived from the tumor suppressor locus in 9q32. *Genes Chromosomes Cancer* 27: 169–176, 2000.
23. Ryle MJ and Hausinger RH. Non-heme iron oxygenases. *Curr Opin Chem Biol* 6: 193–201, 2002.
24. Salnikow K, Davidson T, Zhang Q, Chen LC, Su W, and Costa M. The involvement of hypoxia-inducible transcription factor-1-dependent pathway in nickel carcinogenesis. *Cancer Res* 63: 3524–3530, 2003.
25. Salomons GS, van Dooren SJ, Verhoeven NM, Cecil KM, Ball WS, Degrauw TJ, and Jakobs C. X-linked creatine-transporter gene (SLC6A8) defect: a new creatine-deficiency syndrome. *Am J Hum Genet* 68: 1497–1500, 2001.
26. Semenza GL, Nejfelt MK, Chi SM, and Antonarakis SE. Hypoxia-inducible nuclear factors bind to an enhancer element located 3' to the human erythropoietin gene. *Proc Natl Acad Sci USA* 88: 5680–5684, 1991.
27. Semenza GL, Roth PH, Fang HM, and Wang GL. Transcriptional regulation of genes encoding glycolytic enzymes by hypoxia-inducible factor 1. *J Biol Chem* 269: 23757–23763, 1994.
28. Shoshani T, Faerman A, Mett I, Zelin E, Tenne T, Gorodin S, Moshel Y, Elbaz S, Budanov A, Chajut A, Kalinski H, Kamer I, Rozen A, Mor O, Keshet E, Leshkowitz D, Einat P, Skaliter R, and Feinstein E. Identification of a novel hypoxia-inducible factor 1-responsive gene, RTP801, involved in apoptosis. *Mol Cell Biol* 22: 2283–2293, 2002.
29. Sonna LA, Cullivan ML, Sheldon HK, Pratt RE, and Lilly CM. Effect of hypoxia on gene expression by human hepatocytes (HepG2). *Physiol Genomics* 12: 195–207, 2003.
30. Sowter HM, Ferguson M, Pym C, Watson P, Fox SB, Han C, and Harris AL. Expression of the cell death genes BNip3 and NIX in ductal carcinoma in situ of the breast: correlation of BNip3 levels with necrosis and grade. *J Pathol* 201: 573–580, 2003.
31. Vengellur A and LaPres JJ. The role of hypoxia inducible factor 1 α in cobalt chloride induced cell death in mouse embryonic fibroblasts. *Tox Sci* 82: 638–646, 2004.
32. Vengellur A, Woods BG, Ryan HE, Johnson RS, and LaPres JJ. Gene expression profiling of the hypoxia signaling pathway in hypoxia inducible factor 1 null mouse embryonic fibroblasts. *Gene Expr* 11: 181–197, 2003.
33. Wu Z, Irizarry RA, Gentleman R, Murillo FM, and Spencer F. A Model-Based Background Adjustment for Oligonucleotide Expression Arrays (2004). <http://www.bepress.com/jhubiostat/paper1>.
34. Wykoff CC, Pugh CW, Maxwell PH, Harris AL, and Ratcliffe PJ. Identification of novel hypoxia dependent and independent target genes of the von Hippel-Lindau (VHL) tumour suppressor by mRNA differential expression profiling. *Oncogene* 19: 6297–6305, 2000.